

Being a Bit Frequentist Improves Bayesian Neural Networks

Agustinus Kristiadi
University of Tübingen
agustinus.kristiadi@uni-tuebingen.de

Matthias Hein
University of Tübingen
matthias.hein@uni-tuebingen.de

Philipp Hennig
University of Tübingen and MPI for Intelligent Systems, Tübingen
philipp.hennig@uni-tuebingen.de

Abstract

Despite their compelling theoretical properties, Bayesian neural networks (BNNs) tend to perform worse than frequentist methods in classification-based uncertainty quantification (UQ) tasks such as out-of-distribution (OOD) detection and dataset-shift robustness. In this work, based on empirical findings in prior works, we hypothesize that this issue is due to the avoidance of Bayesian methods in the so-called “OOD training”—a family of techniques for incorporating OOD data during training process, which has since been an integral part of state-of-the-art frequentist UQ methods. To validate this, we treat OOD data as a first-class citizen in BNN training by exploring four different ways of incorporating OOD data in Bayesian inference. We show in extensive experiments that OOD-trained BNNs are competitive to, if not better than recent frequentist baselines. This work thus provides strong baselines for future work in both Bayesian and frequentist UQ.

1 Introduction

Uncertainty quantification (UQ) allows learning systems to “know when they do not know”. It is an important functionality, especially in safety-critical applications of AI (Amodei et al., 2016), where a system encountering a novel task (which should be associated with high uncertainty) should hesitate or notify a human supervisor. Both the Bayesian and frequentist deep learning communities address similar UQ functionality (in particular out-of-distribution (OOD) detection and dataset-shift (DS) robustness), but it appears that even recent Bayesian neural networks (BNNs, Osawa et al., 2019; Tomczak et al., 2020; Dusenberry et al., 2020, etc.) tend to underperform compared to the state-of-the-art frequentist UQ methods (Hendrycks et al., 2019; Lee et al., 2018; Hein et al., 2019; Meinke and Hein, 2020; Bitterwolf et al., 2020, etc.), which generally leverage the so-called *OOD training*: a class of methods where OOD data are used for training. Figure 1 shows this observation in two standard benchmarks for DS robustness (Ovadia et al., 2019) and OOD detection: In both benchmarks, the popular OOD-trained frequentist method OE (Hendrycks et al., 2019) performs much better than BNNs and even Deep Ensemble (Lakshminarayanan et al., 2017), which has been considered as a strong baseline in Bayesian deep learning community (Ovadia et al., 2019).

This paper is thus dedicated to answer the question of “how can we bring the performance of BNNs on par with that of recent frequentist UQ methods?”. Our working hypothesis is that the disparity between them is *not* due to some fundamental advantage of the frequentist viewpoint, but to the more mundane practical fact that recent frequentist UQ methods leverage OOD training. The benefits of this technique are well-studied, both for improving generalization (Zhang and LeCun, 2017) and more recently, for OOD detection (Lee et al., 2018; Hein et al., 2019; Meinke and Hein, 2020; Bitterwolf et al., 2020). But while OOD data have been used for tuning the hyperparameters

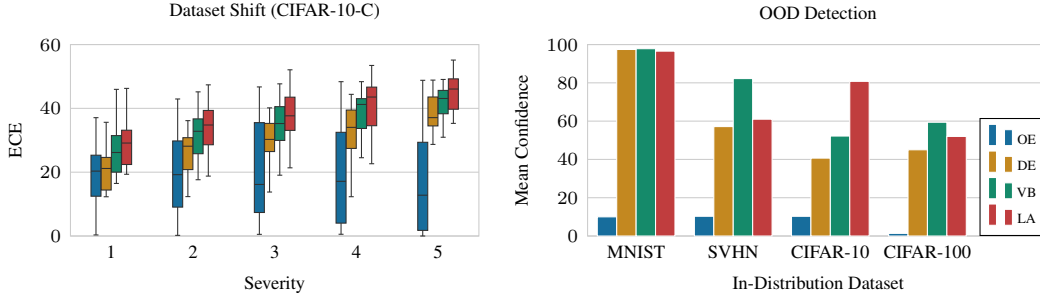


Figure 1: **Left:** Dataset-shift performance in terms of expected calibration error (ECE, Naeini et al., 2015) on the corrupted CIFAR-10 dataset (CIFAR-10-C, Hendrycks and Dietterich, 2019), following Ovadia et al. (2019). **Right:** Average confidence on uniform OOD test data for each in-distribution dataset. LA, VB, DE, and OE stand for the Laplace approximation (MacKay, 1992), variational Bayes (Hinton and Van Camp, 1993), Deep Ensemble (Lakshminarayanan et al., 2017), and Outlier Exposure (Hendrycks et al., 2019), respectively. LA, VB, and DE do not employ OOD training, unlike OE (but it has never seen uniform noises during training). OE is the best-performing method in both cases.

of BNNs (Kristiadi et al., 2020a), it appears that even recently proposed deep Bayesian methods (Swiatkowski et al., 2020; Tomczak et al., 2020; Dusenberry et al., 2020) have not considered OOD training. A reason for this may be because of that it is unclear how can one can incorporate OOD data in the Bayesian inference itself.

In this work, we explore four options—some are philosophically clean, others are heuristics—of incorporating OOD data to Bayesian inference. These methods are motivated by the assumptions that the data (i) have an extra “none” class, (ii) are entirely represented by “soft” labels, (iii) have mixed “hard” and “soft” labels. Last but not least, we also (iv) investigate an interpretation of the popular OE loss as a likelihood which can readily be used in a Bayesian inference. We compare the four of them against strong baselines in various OOD and DS tasks and show that BNNs equipped with these likelihoods can outperform OOD-trained frequentist baseline. Our empirical findings thus validate the hypothesis and we hope that the proposed approaches can serve as strong baselines for future work in both the Bayesian and frequentist deep learning communities.

2 Preliminaries

We focus on classification tasks. Let $F : \mathbb{R}^n \times \mathbb{R}^d \rightarrow \mathbb{R}^c$ defined by $(x, \theta) \mapsto F(x; \theta)$ be an ℓ -layer, c -class NN with any activation function. Here, \mathbb{R}^n , \mathbb{R}^d , and \mathbb{R}^c are the input, parameter, and output spaces of the network, respectively. Let $P(X)$ and $P(Y|X)$ be probability distributions over \mathbb{R}^n and $\{1, \dots, c\}$, respectively. Given an i.i.d. dataset $\mathcal{D} := \{(x^{(i)}, y^{(i)}) : x^{(i)} \sim P(X), y^{(i)} \sim P(Y|X = x^{(i)})\}_{i=1}^m$, the standard training procedure amounts (from the Bayesian perspective) to *maximum a posteriori (MAP) estimation* under a given likelihood $p(\mathcal{D}|\theta)$ and prior $p(\theta)$.

Let Δ^c be the $(c - 1)$ -probability simplex. We define the *softmax* inverse-link function $\sigma : \mathbb{R}^c \rightarrow \Delta^c$ by $\sigma_k(z) := \exp(z_k / \sum_{i=1}^c \exp(z_i))$ for each $k = 1, \dots, c$. A common choice of likelihood function for c -class classification networks is the softmax-Categorical likelihood: Given a data pair $(x, y) \in \mathcal{D}$ and parameter θ , the mapped output $\sigma(F(x; \theta))$ can be interpreted as a probability vector and the *Categorical log-likelihood* over it can be defined by $\log p_{\text{Cat}}(y|x, \theta) := \log \sigma_{y_k}(F(x; \theta))$, i.e. it is simply the logarithm of the y_k -th component of the network’s softmax output. Considering all the data, we write $\log p_{\text{Cat}}(\mathcal{D}|\theta) := \sum_{i=1}^m \log p_{\text{Cat}}(y^{(i)}|x^{(i)}, \theta)$. Then, given a prior $p(\theta)$, the MAP estimate is a particular θ satisfying $\arg \max_{\theta} \log p_{\text{Cat}}(\mathcal{D}|\theta) + \log p(\theta) = \arg \max_{\theta} \log p(\theta|\mathcal{D})$. In the case of a zero-mean isotropic Gaussian prior, this corresponds to a maximum likelihood estimate under a weight decay regularization.

While MAP-estimated networks are established to achieve high accuracy, they are overconfident (Nguyen et al., 2015). Bayesian methods promise to mitigate this issue (Kristiadi et al., 2020a). The core idea of *Bayesian neural networks (BNNs)* is to infer the full posterior $p(\theta|\mathcal{D})$ (instead of just a

single estimate in the case of MAP estimation) and marginalizing it to obtain the predictive distribution $p(y|x) = \int \sigma(F(x; \theta)) p(\theta|\mathcal{D}) d\theta$. Unfortunately, due to the nonlinearity of F in θ , this exact posterior is intractable, and various approximations have been proposed. Prominent among them are variational Bayes (VB, Hinton and Van Camp, 1993; Graves, 2011; Blundell et al., 2015, etc.) and Laplace approximations (LAs, MacKay, 1992; Ritter et al., 2018, etc.). Once the approximate posterior $q(\theta|\mathcal{D}) \approx p(\theta|\mathcal{D})$ has been chosen, one can easily use it to approximate $p(y|x)$ via Monte Carlo (MC) integration.

3 Why BNNs Underperform: A Hypothesis

Let U be the *data region*, i.e. a subset of the input space \mathbb{R}^n where the data distribution $P(X)$ assigns non-negligible mass. Suppose $V := \mathbb{R}^n \setminus U$ is the remaining subset of the input space \mathbb{R}^n that has low probability under $P(X)$, i.e. it is the *OOD region*. It has recently been shown that any point estimate of F can induce an arbitrarily overconfident prediction on V (Hein et al., 2019; Nguyen et al., 2015). While Bayesian methods have been shown to “fix” this issue in the asymptotic regime (i.e. when the distance between a test point $x \in V$ and the data region U tends to infinity Kristiadi et al., 2020a;b), no such guarantee has been shown for *non-asymptotic* regime which contains outliers that are relatively close to U . In fact, empirical evidence shows that Bayesian methods often yield suboptimal results in this regime, as Fig. 1 shows.

In an adjacent field, the frequentist community has proposed a technique, referred to here as *OOD training*, to address this issue. The core idea is to “expose” the network to a particular kind OOD data and let it generalize to unseen outliers. Suppose $\mathcal{D}_{\text{out}} := \{\hat{x}_i \in V\}_{i=1}^{m_{\text{out}}}$ is a collection of m_{out} points sampled from some distribution over V . Then, one can incorporate these OOD samples into the standard MAP objective via an additional objective function \mathcal{L} that depends on the network and \mathcal{D}_{out} , but not the dataset \mathcal{D} . We thus have the following optimization problem:

$$\arg \max_{\theta} \log p_{\text{Cat}}(\mathcal{D}|\theta) + \log p(\theta) + \mathcal{L}(F, \theta, \mathcal{D}_{\text{out}}). \quad (1)$$

For instance, Lee et al. (2018) and Hendrycks et al. (2019) define \mathcal{L} to be the negative expected KL-divergence, and the negative cross-entropy between the softmax output of F under \mathcal{D}_{out} and the uniform discrete distribution, respectively. Intuitively, OOD training’s optimization problem tries to find a parameter vector of F that induces well-calibrated predictions both inside and outside of U . In particular, ideally, the network should retain the performance of the MAP estimate in U , while attaining the maximum entropy or uniform confidence prediction everywhere in V . Empirically, this frequentist robust training scheme obtains state-of-the-art performance in UQ tasks. More specifically, recent literature (e.g. Meinke and Hein, 2020; Bitterwolf et al., 2020) suggests that Outlier Exposure (OE) (Hendrycks et al., 2019) is among the most popular high-performing methods.

While some works have employed OOD data for tuning the hyperparameters of BNNs (Kristiadi et al., 2020a;b), ultimately OOD data are not considered as a first-class citizen in the Bayesian inference itself. Furthermore, while one can argue that BNNs can automatically assign low uncertainty over V and thus robust to outliers, as we have previously discussed, empirical evidence suggests otherwise. Altogether, it thus now seems likely that indeed the fact that BNNs are not exposed to OOD data during training is a major factor contributing to the discrepancy in their UQ performance compared to that of the state-of-the-art frequentist methods like OE.

4 OOD Training for BNNs

Motivated by the hypothesis laid out in the previous section, our goal here is to come up with an OOD training scheme for standard BNN inference while retaining a reasonable Bayesian interpretation. To this end, we explore four different ways of incorporating OOD data in Bayesian inference by making different assumptions about the data and hence the likelihood, starting from the most philosophically clean to the most heuristic.¹

¹One might be tempted to treat \mathcal{L} in (1) as a log-prior. However not only does this mean that we have a (controversial) data-dependent prior, but also it introduces implementation issues, e.g. the KL-divergence term in VB’s ELBO cannot be computed easily anymore.

Method 1: Extra “None” Class

The most straightforward yet philosophically clean way to incorporate unlabeled OOD data is by adding an extra class, corresponding to the “none” class—also known as the “dustbin” or “garbage” class (Zhang and LeCun, 2017). That is, we redefine our network F as a function $\mathbb{R}^n \times \mathbb{R}^{d+\hat{d}} \rightarrow \mathbb{R}^{c+1}$ where \hat{d} is the additional parameters associated with the extra class. Note that this is different to the “background class” method (Zhang and LeCun, 2017; Wang and Aitchison, 2021) which assumes that the extra class is tied to the rest of the classes and thus does not have additional parameters. We choose to use the “dustbin” class since Zhang and LeCun (2017) showed that it is the better of the two.

Under this assumption, we only need to label all OOD data in \mathcal{D}_{out} with the class $c+1$ and add them to the true dataset \mathcal{D} . That is, the new dataset is $\tilde{\mathcal{D}} := \mathcal{D} \amalg \{(x_{\text{out}}^{(1)}, c+1), \dots, (x_{\text{out}}^{(m_{\text{out}})}, c+1)\}$, where \amalg denotes disjoint union. Under this setting, we can directly use the Categorical likelihood and thus, a Bayesian treatment under this assumption has a sound Bayesian interpretation.

Method 2: Soft Labels

In this method, we simply assume that the data have “soft labels”, i.e. the labels are treated as general probability vectors, instead of restricted to integer labels (Thiel, 2008).² Since in this case the labels are instances of compositional data (Aitchison, 1982), we can assume that the target Y is a Δ^c -valued random variable.

Let us first give a soft-label treatment to the original dataset \mathcal{D} . Under this assumption, since one-hot vectors are also elements of Δ^c (they represent the c corners of Δ^c), we do not have to redefine \mathcal{D} other than to one-hot encode the original integer labels. Let us, therefore, denote the one-hot encoded dataset \mathcal{D} by \mathcal{D}_1 . Now let us turn our attention to the OOD training data. The fact that these data should be predicted with maximum entropy suggests that the suitable label for any $x_{\text{out}} \in \mathcal{D}_{\text{out}}$ is the uniform probability vector $u := (1/c, \dots, 1/c)$ of length c —the center of Δ^c . Therefore, we can redefine \mathcal{D}_{out} as the set $\{(x_{\text{out}}^{(1)}, u), \dots, (x_{\text{out}}^{(m_{\text{out}})}, u)\}$, and then define a new dataset $\tilde{\mathcal{D}} := \mathcal{D}_1 \amalg \mathcal{D}_{\text{out}}$ containing both in- and out-distribution training data. Note that without the assumption that Y is a simplex-valued r.v., we cannot encode u as the uniform probability vector, and thus we cannot naturally convey our intuition that we should be maximally uncertain over OOD data.

Under this assumption, we have to adapt the likelihood. A straightforward choice for simplex-valued r.v.s. is the Dirichlet likelihood $p_{\text{Dir}}(y|x, \theta) := \text{Dir}(y|\alpha(F(x; \theta)))$ where we make the dependence of α to the network output $F(x; \theta)$ explicit. So, we obtain the log-likelihood function

$$\log p_{\text{Dir}}(y|x, \theta) = \log \Gamma(\alpha_0) + \sum_{k=1}^c (\alpha_k(F(x; \theta)) - 1) \log y_k - \log \Gamma(\alpha_k(F(x; \theta))), \quad (2)$$

where $\alpha_0 := \sum_{k=1}^c \alpha_k(F(x; \theta))$. Therefore, the log-likelihood for $\tilde{\mathcal{D}}$ is given by $\log p_{\text{Dir}}(\tilde{\mathcal{D}}|x, \theta) = \sum_{i=1}^m \log p_{\text{Dir}}(y^{(i)}|x^{(i)}, \theta) + \sum_{i=1}^{m_{\text{out}}} \log p_{\text{Dir}}(u|x_{\text{out}}^{(i)}, \theta)$, which can readily be used in a Bayesian inference.

One thing left to discuss is the definition of $\alpha(F(x; \theta))$. An option is to decompose it into mean and precision (Minka, 2000). We do so by writing $\alpha_k(F(x; \theta)) = \gamma \sigma_k(F(x; \theta))$ for each $k = 1, \dots, c$, where γ is the precision (treated as a hyperparameter) and the softmax output $\sigma(F(x; \theta))$ represents the mean—which is valid since it is an element of Δ^c . The benefits are two-fold: First, since we focus solely on the mean, it is easier for optimization (Minka, 2000). Indeed, we found that the alternatives, such as $\alpha_k(F(x; \theta)) = \exp(F_k(x; \theta))$ and $\alpha_k(F(x; \theta)) = \log(1 + \exp(F_k(x; \theta)))$, yield worse results. Second, after training, we can use the softmax output of F as usual without additional steps, i.e. when making prediction, we can treat the network as if it was trained using the standard softmax-Categorical likelihood.

²The term “soft label” here is different than “fuzzy label” (Kuncheva, 2000; El Gayar et al., 2006) where it is not constrained to sum to one.

Method 3: Mixed Labels

There is a technical issue when using the Dirichlet likelihood for the in-distribution data: It is known that the Dirichlet likelihood does not work well with one-hot encoded vectors and harder to optimize than the Categorical likelihood (Malinin and Gales, 2018). To see this, notice in (2) that the logarithm is applied on y_k , in contrast to $\sigma_k(F(x; \theta))$ in the Categorical likelihood. If y is a one-hot encoded vector, this implies that for all but one $k \in \{1, \dots, c\}$, the expression $\log y_k$ is undefined and thus the entire log-likelihood also is. While one can mitigate this issue via e.g. label smoothing (Malinin and Gales, 2018; Szegedy et al., 2016), ultimately we found that models with the Dirichlet likelihood generalize worse than their Categorical counterparts (more in Section 6). Fortunately, the Dirichlet log-likelihood (2) does not suffer from this issue when used for OOD data because their label u is the uniform probability vector—in particular, all components of u are strictly larger than zero.

Motivated by these observations, we combine the best of best worlds in the stability of the Categorical likelihood in modeling “hard” one-hot encoded labels (or equivalently, integer labels) and the flexibility of the Dirichlet likelihood in modeling soft labels. To this end, we assume that all the in-distribution data in \mathcal{D} have the standard integer labels, while all the OOD data in \mathcal{D}_{out} have soft labels. Then, assuming that \mathcal{D} and \mathcal{D}_{out} are independent, we define the following “mixed” log-likelihood:

$$\log p(\mathcal{D}, \mathcal{D}_{\text{out}}|\theta) := \sum_{i=1}^m \log p_{\text{Cat}}(y^{(i)}|x^{(i)}, \theta) + \sum_{i=1}^{m_{\text{out}}} \log p_{\text{Dir}}(u|x_{\text{out}}^{(i)}, \theta)$$

The implicit assumption of this formulation is that, unlike the two previous methods, we have two distinct generative processes for generating the labels of input points in U and V . Data in \mathcal{D} can thus have a different “data type” than data in \mathcal{D}_{out} . This method can therefore be interpreted as solving a multi-task or multi-modal learning problem.

Method 4: Frequentist-Loss Likelihood

Considering the effectiveness of frequentist UQ methods, it is, therefore, tempting to give a direct Bayesian treatment upon them. But to do so, we first have to find a sound probabilistic justification of (1) since not all loss functions can be interpreted as likelihood functions. We use the popular OE objective (Hendrycks et al., 2019) as a use case.

First, recall that OE’s OOD objective—the last term in (1)—is given by

$$\mathcal{L}_{\text{OE}} := - \mathbb{E}_{x_{\text{out}} \sim \mathcal{D}_{\text{out}}} (H(\sigma(F(x_{\text{out}}; \theta)), u)) = \frac{1}{c m_{\text{out}}} \sum_{i=1}^{m_{\text{out}}} \sum_{k=1}^c \log \sigma_c(F(x_{\text{out}}^{(i)}; \theta)), \quad (3)$$

where $u := (1/c, \dots, 1/c) \in \Delta^c$ is the uniform probability vector of length c and H is the functional measuring the *cross-entropy* between its two arguments. Our goal here is to interpret (3) as a log-likelihood function: we aim at finding a log-likelihood function $\log p(\mathcal{D}_{\text{out}}|\theta)$ over \mathcal{D}_{out} that has the form of \mathcal{L}_{OE} . This is sufficient for defining the overall likelihood over \mathcal{D} and \mathcal{D}_{out} since given this function and assuming that these datasets are independent, we readily have a probabilistic interpretation of the log-likelihood terms in (1): $\log p(\mathcal{D}, \mathcal{D}_{\text{out}}|\theta) = \log p_{\text{Cat}}(\mathcal{D}|\theta) + \log p(\mathcal{D}_{\text{out}}|\theta)$.

We begin with the assumption that the Categorical likelihood is used to model both the in- and out-of-distribution data—in particular we use the standard integer labels for both \mathcal{D} and \mathcal{D}_{out} . Now, recall that the OOD data ideally have the uniform confidence, that is, they are equally likely under all possible labels. To convey this, we redefine the OOD dataset \mathcal{D}_{out} by assigning all c possible labels to each x_{out} :

$$\mathcal{D}_{\text{out}} := \{(x_{\text{out}}^{(1)}, 1), \dots, (x_{\text{out}}^{(1)}, K), \dots, (x_{\text{out}}^{(m_{\text{out}})}, 1), \dots, (x_{\text{out}}^{(m_{\text{out}})}, K)\}. \quad (4)$$

Thus, given m_{out} unlabeled OOD data, we have $|\mathcal{D}_{\text{out}}| = c m_{\text{out}}$ OOD data points in our OOD training set. So, the negative log-Categorical likelihood over \mathcal{D}_{out} is given by

$$\log p(\mathcal{D}_{\text{out}}|\theta) = \sum_{i=1}^{m_{\text{out}}} \sum_{k=1}^c \log \sigma_c(F(x_{\text{out}}^{(i)}; \theta)) \quad (5)$$

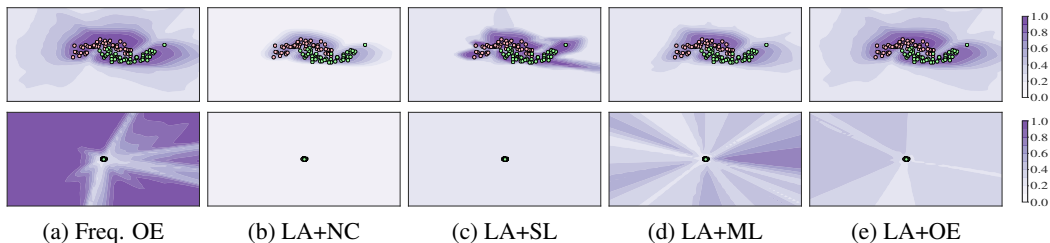


Figure 2: Confidence estimate of the frequentist OE baseline **(a)** and the Bayesian OOD-training methods discussed in Section 4 **(b-e)**. For the BNNs, we use the Laplace approximation (LA). The suffixes “+NC”, “+SL”, “+ML”, and “+OE” refer to the none-class, soft-labels, mixed-labels, and OE likelihoods, respectively. The bottom row shows the zoomed-out versions of the top one.

Comparing this to (3), we identify that $\log p(\mathcal{D}_{\text{out}}|\theta)$ is exactly \mathcal{L}_{OE} , up to a constant factor $\frac{1}{c m_{\text{out}}}$, which can be thought as a tempering factor to $p(\mathcal{D}_{\text{out}}|\theta)$. We have thus obtained the probabilistic interpretation of OE’s objective—this likelihood can then be soundly used in a Bayesian inference—albeit arising from a heuristic assumption about the data (4).

4.1 Discussion

Here, we discuss the question of whether there is an inherent advantage of using OOD-trained BNNs instead of the standard OOD-trained network. One answer to this question is given by the recent finding that Bayesian methods naturally yield low uncertainty in regions far away from the data region (Kristiadi et al., 2020a). In contrast, OOD-trained point-estimated networks do not enjoy such a guarantee by default and must resort to e.g. generative models (Meinke and Hein, 2020). We illustrate this observation synthetically in Fig. 2.

5 Related Work

OOD training for BNNs has recently been used for tuning the hyperparameters of LAs (Kristiadi et al., 2020a; 2021). However, it appears that OOD data have not been treated as first-class citizens in the Bayesian inference itself. From an adjacent field, adversarial training for BNNs have also recently been studied. In particular, Liu et al. (2019) specifically employ VB and modify the first term of the ELBO to take into account the worst-case perturbation of each data point, which can be thought of as a particular type of OOD data. Unlike theirs, our method is agnostic to the approximate inference method used.

Non-Bayesian Dirichlet-based models have recently been studied for UQ (Sensoy et al., 2018). Similar to our proposed likelihood, Malinin and Gales (2018; 2019); Nandy et al. (2020) use the Dirichlet likelihood to model the output of a network and employ OOD training in a non-Bayesian fashion. Indeed, they employ a custom, non-standard loss, and thus their method’s Bayesian interpretation is unclear. In contrast, for modeling soft labels, we simply use the standard Dirichlet log-likelihood function—which is well-studied in the context of generalized linear models (Gueorguieva et al., 2008)—thus retaining the clear Bayesian interpretation of non-OOD-trained BNNs.

6 Experiments

6.1 Setup

Baselines We use the following strong, recent baselines to represent non-Bayesian methods: (i) standard MAP-trained network (**MAP**), (ii) Deep Ensemble (**DE**, Lakshminarayanan et al., 2017), and (iii) Outlier Exposure (**OE**, Hendrycks et al., 2019). Note that DE and OE are among the established state-of-the-art non-Bayesian methods in DS robustness (Ovadia et al., 2019) and OOD detection (Meinke and Hein, 2020; Bitterwolf et al., 2020), respectively. For the standard Bayesian methods, i.e. those considering only \mathcal{D} in the inference, we use (iv) the all-layer diagonal Laplace approximation on top of the MAP network (**LA**) and (v) the last-layer mean-field VB (**VB**, Graves,

2011; Blundell et al., 2015). We deliberately use only these simple Bayesian methods to validate that the proposed likelihood could make even these crudely approximated BNNs competitive to the strong baselines. Finally, to represent our methods, we again use same LA and VB but with the modifications proposed in Section 4. We denote these modified methods **LA+X** and **VB+X**, respectively. Here, **X** is the abbreviation for the proposed methods, i.e. **NC** for the none-class method (Method 1), **SL** for the soft label method (Method 2), **ML** for the mixed-label method (Method 3), and **OE** for the “OE likelihood” (Method 4).

Datasets As the in-distribution datasets, we use: (i) MNIST, (ii) Fashion-MNIST (F-MNIST, Xiao et al., 2017), (iii) SVHN, (iv) CIFAR-10, and (v) CIFAR-100. For each of them, we obtain a validation set of size 2000 by randomly splitting the test set. For methods requiring OOD training data, i.e. OE, LA+X, and VB+X, we use the 32x32 downsampled ImageNet dataset (Chrabaszcz et al., 2017) as an alternative to the 80M Tiny Images dataset used by Hendrycks et al. (2019); Meinke and Hein (2020), since the latter is not available anymore. For OOD detection tasks, we use various *unseen* (i.e. not used for training or tuning) OOD test sets as used in (Meinke and Hein, 2020; Hein et al., 2019), both real-world (e.g. E-MNIST) and synthetic (e.g. uniform noise). Meanwhile, for DS robustness tasks, we use the standard benchmark tasks (Ovadia et al., 2019; Hendrycks and Dietterich, 2019): the corrupted CIFAR-10 dataset (CIFAR-10-C). Finally, for text classification, we use (i) the 20-Newsgroups (20NG) dataset, (ii) Stanford Sentiment Treebank (SST, Socher et al., 2013), and (iii) the TREC dataset (Voorhees, 2001). We detail of all OOD test sets in Appendix A.1.

Metrics To measure OOD detection performance, we use the standard FPR95 metric, which measures the false positive rate at 95% true positive rate. Other metrics such as mean confidence and area under ROC curve (Hendrycks and Gimpel, 2017) are presented in the appendix. Meanwhile, to measure DS robustness and predictive performance, we use test accuracy, test negative log-likelihood (NLL), the Brier score (Brier, 1950), and expected calibration error (ECE) with 15 bins (Naeini et al., 2015).

Training—Non-Bayesian For MNIST and F-MNIST, we use a five-layer LeNet architecture. Meanwhile, for SVHN, CIFAR-10, and CIFAR-100, we use WideResNet-16-4 (Zagoruyko and Komodakis, 2016). For all methods, the training procedures are as follows. For LeNet, we use Adam with initial learning rate of 1×10^{-3} and annealed it using the cosine decay method (Loshchilov and Hutter, 2017) along with weight decay of 5×10^{-4} for 100 epochs. We use a batch size of 128 for both in- and out-distribution batch, amounting to an effective batch size of 256 in the case of OOD training. The standard data augmentation pipeline (random crop and horizontal flip) is applied to both in-distribution and OOD data. For WideResNet-16-4, we use SGD instead with an initial learning rate of 1×10^{-1} and Nesterov momentum of 0.9 along with the dropout regularization with rate 0.3—all other hyperparameters are identical to LeNet. Finally, we use 5 ensemble members for DE.

Training—Bayesian For both LA, VB, and their variants (i.e. LA+X and VB+X), we use the identical setup as in the non-Bayesian training above. Additionally, for LA and LA+X, we use the diagonal Fisher matrix as the approximate Hessian. Moreover, we tune prior variance by minimizing the validation Brier score. All predictions are done using 20 MC samples. For VB and VB+X, we use a diagonal Gaussian variational posterior for both the last-layer weight matrix and bias vector. Moreover, the prior is a zero-mean isotropic Gaussian with prior precision 5×10^{-4} (to emulate the choice of the weight decay in the non-Bayesian training). The trade-off hyperparameter τ of the ELBO is set to the standard value of 0.1 (Osawa et al., 2019; Zhang et al., 2018). We do not use weight decay on the last layer since the regularization of its parameters is done by the KL-term of the ELBO. Lastly, we use 5 and 200 MC samples for computing the ELBO and for making predictions, respectively.

6.2 Generalization and Calibration

We present the generalization and calibration performance in Table 1. We note that generally, all methods discussed in Section 4 attain comparable accuracy to and are better calibrated than the vanilla MAP/OE models. However, the “soft label” method tends to underperform in both accuracy and ECE—this can be seen clearly on CIFAR-100. This issue appears to be because of the numerical issue we have discussed in Section 4. Note that this issue seems to also plague other Dirichlet-based methods such as Prior Networks (Malinin and Gales, 2018; 2019), cf. Appendix A. Overall, it

Table 1: Test accuracy / ECE, averaged over five prediction runs. Best values of each categories (baselines, VB, LA) are in bold.

Methods	MNIST	F-MNIST	SVHN	CIFAR-10	CIFAR-100
MAP	99.4/6.4	92.4/13.9	97.4/8.9	94.8/10.0	76.7/14.3
DE	99.5 /8.6	93.6 / 3.6	97.6 / 3.5	95.7 / 4.5	80.0 / 1.9
OE	99.4/ 5.3	92.3/12.1	97.4/10.6	94.6/13.2	76.7/15.0
VB	99.5 /11.2	92.4/3.7	97.5/5.7	94.9/5.8	75.4 / 8.3
+NC	99.4/12.6	92.2/3.3	97.5/ 4.1	94.4/5.5	74.1/10.7
+SL	99.5 /10.5	93.1 /6.3	97.6 /9.3	93.0/11.0	71.4/13.0
+ML	99.3/11.8	92.0/2.5	97.6 /4.2	95.0 /4.9	75.4 /10.4
+OE	99.4/ 10.0	92.3/3.0	97.6 /5.7	94.8/ 4.6	74.2/8.9
LA	99.4/7.6	92.5/11.3	97.4/3.3	94.8 /7.5	76.6/8.3
+NC	99.4/5.4	92.4/8.5	97.3/4.6	94.0/ 6.6	76.2/6.1
+SL	99.7 /12.1	93.2 / 3.2	97.5 /7.4	93.6/10.2	72.3/7.1
+ML	99.4/7.5	92.5/5.9	97.4/ 2.9	94.8 /6.9	76.5/ 4.4
+OE	99.4/ 4.8	92.3/7.4	97.4/3.2	94.6/8.8	76.7 / 4.4

Table 2: OOD data detection in terms of the FPR95 metric. Values are averages over six OOD test datasets and five prediction runs—lower is better. Best values of each categories (baselines, VB, LA) are in bold.

Methods	MNIST	F-MNIST	SVHN	CIFAR-10	CIFAR-100
MAP	17.7	69.4	22.4	52.4	81.0
DE	10.6	61.4	10.1	32.3	73.3
OE	5.4	16.2	2.1	22.8	54.0
VB	25.7	63.3	22.0	36.5	77.6
+NC	7.5	15.0	1.4	28.0	49.9
+SL	2.7	4.2	1.8	40.4	62.3
+ML	7.4	19.6	1.4	29.1	50.2
+OE	6.8	22.4	1.5	29.8	53.3
LA	19.4	68.7	17.1	53.6	81.3
+NC	6.6	8.3	1.5	20.1	47.4
+SL	2.2	4.1	1.0	38.5	60.9
+ML	5.5	14.3	1.1	21.8	52.5
+OE	5.4	17.0	1.1	23.3	53.9

appears that Bayesian OOD training with NC, ML, and OE is not harmful to the in-distribution performance—they are even more calibrated than the frequentist OE.

6.3 OOD Detection

We present the OOD detection results on image classification datasets in Table 2. As indicated in Fig. 1, OE is on average significantly better than even DE, while being much cheaper since OE is a single-model method. The vanilla Bayesian baselines, represented by VB and LA, achieve worse results than DE (and thus OE). But, when OOD training is employed to train these BNNs using the four methods we considered in Section 4, their performance improves. We observe that all Bayesian OOD training methods generally yield better results than DE and become competitive to OE. In particular, while the “soft-label” method (SL) is best for simple datasets (MNIST, F-MNIST), we found that the simplest “none class” method (NC) achieves the best results as a whole, when considering all in-distribution data. In Table 3, we additionally show the results on text classification datasets (detailed results in Appendix A). We found that the OOD training methods consistently improve both the calibration and OOD-detection performance of the vanilla Bayesian methods, making them on par with OE. As before, the “none class” method performs the best in OOD detection. This is a reassuring result since NC is also the most philosophically clean (i.e. requires fewer heuristics) than other Bayesian OOD-training methods considered.

Table 3: OOD data detection on text classification tasks. Values are FPR95, averaged over three OOD test datasets and five prediction runs. Detailed values are in Table 10 (appendix).

Methods	ECE			FPR95		
	SST	20NG	TREC	SST	20NG	TREC
MAP	20.8	19.3	17.2	100.0	0.0	96.3
DE	2.5	9.3	10.6	100.0	0.6	24.2
OE	13.0	20.1	9.4	0.0	0.0	0.0
LA	21.0	18.9	17.3	100.0	0.0	96.4
+NC	17.9	16.5	18.6	0.0	0.0	0.0
+SL	17.5	19.4	10.4	95.3	0.0	0.8
+ML	11.4	18.2	11.5	84.6	0.0	0.0
+OE	12.8	19.8	8.4	0.0	0.0	0.0

Table 4: OOD data detection under models trained with synthetic noises (Hein et al., 2019) as \mathcal{D}_{out} . Values are FPR95, averaged over five prediction runs and all OOD test datasets—lower is better.

Methods	MNIST	F-MNIST	SVHN	CIFAR-10	CIFAR-100
OE	7.7	31.1	11.4	31.0	60.1
LA	19.4	68.7	17.1	53.6	81.3
+NC	9.0	30.5	10.5	26.4	64.5
+SL	2.7	11.3	93.7	37.9	68.6
+ML	7.7	24.9	14.4	28.4	61.0
+OE	7.7	31.3	10.1	35.3	56.4

Last but not least, a common concern regarding OOD training is the choice of \mathcal{D}_{out} . As an attempt to address this, in Table 4 we provide results on OOD detection when the model is trained using a synthetic noise dataset, instead of the 32x32 ImageNet dataset. The noise dataset used here is the “smooth noise” dataset (Hein et al., 2019), obtained by permuting, blurring, and contrast-rescaling the original training dataset. We found that even with such a simple dataset, we can still generally obtain better results than the frequentist OE baseline.

6.4 Dataset-Shift Robustness

In this family of UQ tasks, it has previously been shown that DE obtains the state-of-the-art performance (Ovadia et al., 2019). Indeed, as can be seen in Fig. 3, DE generally outperforms the standard MAP model and vanilla Bayesian methods (LA, VB). However, OOD-training changes this outcome: When trained with OOD data, both the MAP³ and Bayesian models significantly outperform DE in almost all metrics considered. Note that this improvement is not solely because of the OOD data: the OOD-trained non-Bayesian OE generally performs worse than the OOD-trained Bayesian methods. This indicates that *both* being Bayesian and considering OOD data during training are required to obtain these good results.

Even though it is the best in OOD detection, here we observe that NC is less calibrated than its counterparts in terms of calibration. This might be due to the “incompatibility” of calibration metrics with the additional class: When the data are corrupted, they become closer to the OOD data, and thus NC tends to assign higher probability mass to the last class which does not correspond to any of the true classes (contrast this to other the approaches). Therefore, in this case, the confidence over the true class becomes necessarily lower—more so than the other approaches. Considering that calibration metrics depend on the confidence of the true class, the calibration of NC thus suffers. One way to overcome this issue is to make calibration metrics aware of the “none class”, e.g. by measuring calibration on data that have low “none class” probability. We left the investigation for interesting future research.

³We can consider OE as an OOD-trained MAP network.

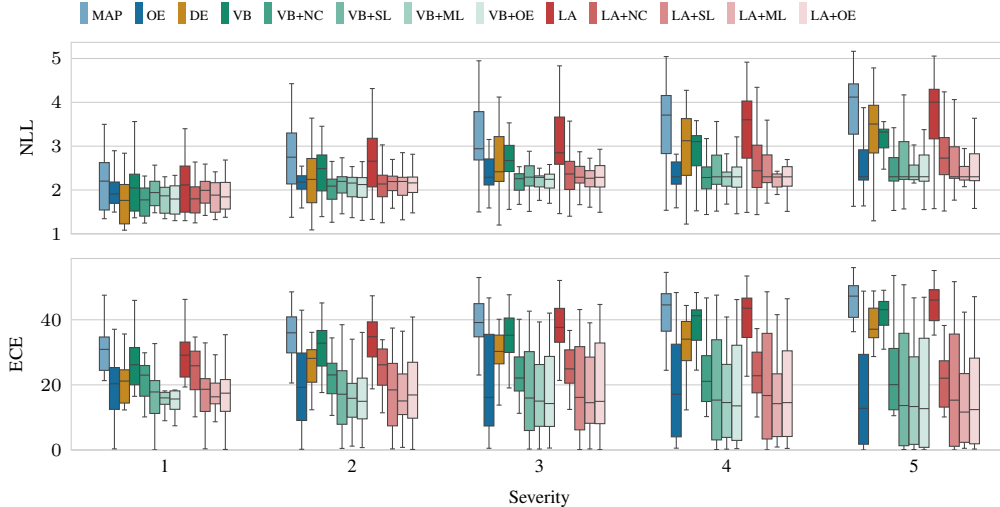


Figure 3: Dataset shift performance on the CIFAR-10-C dataset in terms of NLL and ECE (lower is better for both metrics) at each severity levels.

6.5 Costs

The additional costs associated with the OOD-training methods are negligible: Like other non-Bayesian OOD-training methods, the only overhead is the additional minibatch of OOD training data at each training iteration. That is, these costs are similar to when considering training with double the minibatch size. In the particular case of LA, additionally, there is another overhead: In its Hessian computation, one effectively computes it with twice the number of the original data. However, this is a non-issue since it is standard to minibatch the Hessian computation, and it only needs to be done once after training.

7 Conclusion

We raised an important observation regarding contemporary BNNs’ performance in uncertainty quantification, in particular in dataset-shift robustness and OOD detection tasks. We noticed that BNNs tend to underperform compared to non-Bayesian UQ methods. Based on this observation, we hypothesized that this issue is due to the fact that recent frequentist UQ methods utilize an auxiliary OOD training set. To validate this hypothesis, we explored ways to incorporate OOD training data into BNNs while still maintaining a reasonable Bayesian interpretation. Our experimental results showed that imbuing BNN training with OOD data significantly improved the performance of BNNs, making them competitive or even better than non-Bayesian counterparts. In particular, we found that the most philosophically Bayesian-compatible way of OOD training performs best. We hope that the studied methods can be strong baselines for future work in Bayesian deep learning.

Acknowledgments

The authors gratefully acknowledge financial support by the European Research Council through ERC StG Action 757275 / PANAMA; the DFG Cluster of Excellence “Machine Learning - New Perspectives for Science”, EXC 2064/1, project number 390727645; the German Federal Ministry of Education and Research (BMBF) through the Tübingen AI Center (FKZ: 01IS18039A); and funds from the Ministry of Science, Research and Arts of the State of Baden-Württemberg. AK is grateful to the International Max Planck Research School for Intelligent Systems (IMPRS-IS) for support.

References

- Dario Amodei, Chris Olah, Jacob Steinhardt, Paul Christiano, John Schulman, and Dan Mané. Concrete Problems in AI Safety. *arXiv preprint arXiv:1606.06565*, 2016.
- Kazuki Osawa, Siddharth Swaroop, Mohammad Emamiyaz E Khan, Anirudh Jain, Runa Eschenhagen, Richard E Turner, and Rio Yokota. Practical Deep Learning with Bayesian Principles. In *NeurIPS*, 2019.
- Marcin Tomczak, Siddharth Swaroop, and Richard Turner. Efficient Low Rank Gaussian Variational Inference for Neural Networks. In *NeurIPS*, 2020.
- Michael Dusenberry, Ghassen Jerfel, Yeming Wen, Yian Ma, Jasper Snoek, Katherine Heller, Balaji Lakshminarayanan, and Dustin Tran. Efficient and Scalable Bayesian Neural Nets with Rank-1 Factors. In *ICML*, 2020.
- Dan Hendrycks, Mantas Mazeika, and Thomas Dietterich. Deep Anomaly Detection with Outlier Exposure. In *ICLR*, 2019.
- Kimin Lee, Honglak Lee, Kibok Lee, and Jinwoo Shin. Training Confidence-Calibrated Classifiers for Detecting Out-of-Distribution Samples. In *ICLR*, 2018.
- Matthias Hein, Maksym Andriushchenko, and Julian Bitterwolf. Why Relu Networks Yield High-Confidence Predictions Far Away from the Training Data and How to Mitigate the Problem. In *CVPR*, 2019.
- Alexander Meinke and Matthias Hein. Towards Neural Networks that Provably Know when They don't Know. In *ICLR*, 2020.
- Julian Bitterwolf, Alexander Meinke, and Matthias Hein. Certifiably Adversarially Robust Detection of Out-of-Distribution Data. In *NeurIPS*, 2020.
- Yaniv Ovadia, Emily Fertig, Jie Ren, Zachary Nado, David Sculley, Sebastian Nowozin, Joshua Dillon, Balaji Lakshminarayanan, and Jasper Snoek. Can You Trust Your Model's Uncertainty? Evaluating Predictive Uncertainty under Dataset Shift. In *NeurIPS*, 2019.
- Balaji Lakshminarayanan, Alexander Pritzel, and Charles Blundell. Simple and Scalable Predictive Uncertainty Estimation Using Deep Ensembles. In *NIPS*, 2017.
- Mahdi Pakdaman Naeni, Gregory Cooper, and Milos Hauskrecht. Obtaining Well Calibrated Probabilities using Bayesian Binning. In *AAAI*, 2015.
- Dan Hendrycks and Thomas Dietterich. Benchmarking Neural Network Robustness to Common Corruptions and Perturbations. In *ICLR*, 2019.
- David JC MacKay. A Practical Bayesian Framework for Backpropagation Networks. *Neural computation*, 4(3), 1992.
- Geoffrey E Hinton and Drew Van Camp. Keeping the Neural Networks Simple by Minimizing the Description Length of the Weights. In *COLT*, 1993.
- Xiang Zhang and Yann LeCun. Universum Prescription: Regularization Using Unlabeled Data. In *AAAI*, 2017.
- Agustinus Kristiadi, Matthias Hein, and Philipp Hennig. Being Bayesian, Even Just a Bit, Fixes Overconfidence in ReLU Networks. In *ICML*, 2020a.
- Jakub Swiatkowski, Kevin Roth, Bastiaan S Veeling, Linh Tran, Joshua V Dillon, Stephan Mandt, Jasper Snoek, Tim Salimans, Rodolphe Jenatton, and Sebastian Nowozin. The k -tied Normal Distribution: A Compact Parameterization of Gaussian Mean Field Posteriors in Bayesian Neural Networks. In *ICML*, 2020.
- Anh Nguyen, Jason Yosinski, and Jeff Clune. Deep neural networks are easily fooled: High confidence predictions for unrecognizable images. In *CVPR*, 2015.
- Alex Graves. Practical Variational Inference for Neural Networks. In *NIPS*. 2011.
- Charles Blundell, Julien Cornebise, Koray Kavukcuoglu, and Daan Wierstra. Weight Uncertainty in Neural Networks. In *ICML*, 2015.
- Hippolyt Ritter, Aleksandar Botev, and David Barber. A Scalable Laplace Approximation for Neural Networks. In *ICLR*, 2018.

- Agustinus Kristiadi, Matthias Hein, and Philipp Hennig. An Infinite-Feature Extension for Bayesian ReLU Nets That Fixes Their Asymptotic Overconfidence. *arXiv preprint arXiv:2010.02709*, 2020b.
- Xi Wang and Laurence Aitchison. A Statistical Theory of Out-of-Distribution Detection. *arXiv preprint arXiv:2102.12959*, 2021.
- Christian Thiel. Classification on Soft Labels is Robust Against Label Noise. In *International Conference on Knowledge-Based and Intelligent Information and Engineering Systems*, 2008.
- Ludmila Kuncheva. *Fuzzy Classifier Design*. Springer Science & Business Media, 2000.
- Neamat El Gayar, Friedhelm Schwenker, and Günther Palm. A Study of the Robustness of KNN Classifiers Trained Using Soft Labels. In *IAPR Workshop on Artificial Neural Networks in Pattern Recognition*, 2006.
- John Aitchison. The Statistical Analysis of Compositional Data. *Journal of the Royal Statistical Society: Series B (Methodological)*, 44(2), 1982.
- Thomas Minka. Estimating a Dirichlet distribution, 2000.
- Andrey Malinin and Mark Gales. Predictive uncertainty estimation via prior networks. In *NIPS*, 2018.
- Christian Szegedy, Vincent Vanhoucke, Sergey Ioffe, Jon Shlens, and Zbigniew Wojna. Rethinking the Inception Architecture for Computer Vision. In *Proceedings of the IEEE Conference on Computer Vision and Pattern Recognition*, 2016.
- Agustinus Kristiadi, Matthias Hein, and Philipp Hennig. Learnable Uncertainty under Laplace Approximations. In *UAI*, 2021.
- Xuanqing Liu, Yao Li, Chongruo Wu, and Cho-Jui Hsieh. Adv-BNN: Improved Adversarial Defense through Robust Bayesian Neural Network. In *ICLR*, 2019.
- Murat Sensoy, Lance Kaplan, and Melih Kandemir. Evidential deep learning to quantify classification uncertainty. In *NIPS*, 2018.
- Andrey Malinin and Mark Gales. Reverse KL-Divergence Training of Prior Networks: Improved Uncertainty and Adversarial Robustness. In *NIPS*, 2019.
- Jay Nandy, Wynne Hsu, and Mong Li Lee. Towards Maximizing the Representation Gap between In-Domain & Out-of-Distribution Examples. In *NeurIPS*, 2020.
- Ralitza Gueorguieva, Robert Rosenheck, and Daniel Zelterman. Dirichlet Component Regression and Its Applications to Psychiatric Data. *Computational Statistics & Data Analysis*, 52(12), 2008.
- Han Xiao, Kashif Rasul, and Roland Vollgraf. Fashion-MNIST: a Novel Image Dataset for Benchmarking Machine Learning Algorithms. *arXiv preprint arXiv:1708.07747*, 2017.
- Patryk Chrabaszcz, Ilya Loshchilov, and Frank Hutter. A Downsampled Variant of ImageNet as an Alternative to the CIFAR dDatasets. *arXiv preprint arXiv:1707.08819*, 2017.
- Richard Socher, Alex Perelygin, Jean Wu, Jason Chuang, Christopher D Manning, Andrew Y Ng, and Christopher Potts. Recursive Deep Models for Semantic Compositionality Over a Sentiment Treebank. In *EMNLP*, 2013.
- Ellen M Voorhees. Overview of the TREC-9 Question Answering Track. In *Text REtrieval Conference (TREC)*, 2001.
- Dan Hendrycks and Kevin Gimpel. A Baseline for Detecting Misclassified and Out-of-Distribution Examples in Neural Networks. In *ICLR*, 2017.
- Glenn W Brier. Verification of Forecasts Expressed in Terms of Probability. *Monthly Weather Review*, 78(1), 1950.
- Sergey Zagoruyko and Nikos Komodakis. Wide Residual Networks. In *BMVC*, 2016.
- Ilya Loshchilov and Frank Hutter. SGDR: Stochastic Gradient Descent with Warm Restarts. In *ICLR*, 2017.
- Guodong Zhang, Shengyang Sun, David Duvenaud, and Roger Grosse. Noisy Natural Gradient as Variational Inference. In *ICML*, 2018.
- Gregory Cohen, Saeed Afshar, Jonathan Tapson, and Andre Van Schaik. EMNIST: Extending MNIST to Handwritten Letters. In *International Joint Conference on Neural Networks (IJCNN)*, 2017.

- Tarin Clanuwat, Mikel Bober-Irizar, Asanobu Kitamoto, Alex Lamb, Kazuaki Yamamoto, and David Ha. Deep Learning for Classical Japanese Literature. *arXiv preprint arXiv:1812.01718*, 2018.
- Fisher Yu, Ari Seff, Yinda Zhang, Shuran Song, Thomas Funkhouser, and Jianxiong Xiao. LSUN: Construction of a Large-Scale Image Dataset Using Deep Learning with Humans in the Loop. *arXiv preprint arXiv:1506.03365*, 2015.
- Desmond Elliott, Stella Frank, Khalil Sima'an, and Lucia Specia. Multi30K: Multilingual English-German Image Descriptions. In *ACL Workshop on Vision and Language*, 2016.
- Samuel R Bowman, Gabor Angeli, Christopher Potts, and Christopher D Manning. A Large Annotated Corpus for Learning Natural Language Inference. In *EMNLP*, 2015.
- Kyunghyun Cho, Bart Van Merriënboer, Caglar Gulcehre, Dzmitry Bahdanau, Fethi Bougares, Holger Schwenk, and Yoshua Bengio. Learning Phrase Representations Using RNN Encoder-Decoder for Statistical Machine Translation. In *EMNLP*, 2014.

Appendix A Additional Experiment Details

A.1 OOD Test Sets

For image-based OOD detection tasks, we use the following test sets on top of MNIST, F-MNIST, SVHN, CIFAR-10, and CIFAR-100:

- E-MNIST: Contains handwritten letters (“a”-“z”)—same format as MNIST (Cohen et al., 2017).
- K-MNIST: Contains handwritten Hiragana scripts—same format as MNIST (Clanuwat et al., 2018).
- LSUN-CR: Contains real-world images of classrooms (Yu et al., 2015).
- CIFAR-GR: Obtained by converting CIFAR-10 test images to grayscale.
- F-MNIST-3D: Obtained by converting single-channel F-MNIST images into three-channel images—all these three channels have identical values.
- UNIFORM: Obtained by drawing independent uniformly-distributed random pixel.
- SMOOTH: Obtained by permuting, smoothing, and contrast-rescaling the original (i.e. the respective in-distribution) test images (Hein et al., 2019).

Meanwhile, for text classification, we use the following OOD test set, following (Hendrycks et al., 2019):

- MULTI30K: Multilingual English-German image description dataset (Elliott et al., 2016).
- WMT16: Machine-translation dataset, available at <http://www.statmt.org/wmt14/translation-task.html>.
- SNLI: Collection of human-written English sentence pairs manually labeled for balanced classification with the labels entailment, contradiction, and neutral (Bowman et al., 2015).

Finally, for dataset-shift robustness tasks, we use the standard dataset:

- CIFAR-10-C: Contains 19 different perturbations—e.g. snow, motion blur, brightness rescaling—with 5 level of severity for a total of 95 distinct shifts (Hendrycks and Dietterich, 2019; Ovadia et al., 2019).

A.2 Text Classification Setup

The network used is a two-layer Gated Recurrent Unit (GRU, Cho et al., 2014) with 128 hidden units on each layer. The word-embedding dimension is 50 and the maximum vocabulary size is 10000. We put an affine layer on top of the last GRU output to translate the hidden units to output units. Both the LA and VB are applied only on this layer. We use batch size of 64 and Adam optimizer with learning rate of 0.01 without weight decay, except for LA in which case we use weight decay of 5×10^{-4} . The optimization is done for 5 epochs, following (Hendrycks et al., 2019).

A.3 Additional Results

The detailed, non-averaged results for the FPR95 metric are in Table 5. Furthermore, additional results with the area-under-ROC-curve (AUROC), area-under-precision-recall-curve (AUPRC), and mean confidence (MMC) metrics are in Tables 5 to 8, respectively. For the full results of FPR95 with the SMOOTH noise dataset as \mathcal{D}_{out} are in Table 9. Finally, the full results of the NLP experiment is in Table 10.

Table 5: OOD data detection in terms of FPR95. Lower is better. Values are averages over five prediction runs.

Datasets	MAP	OE	DE	VB						LA					
				Plain	NC1	NC2	SL	ML	OE	Plain	NC1	NC2	SL	ML	OE
MNIST															
F-MNIST	11.8	0.0	5.3	12.5	0.1	0.0	0.0	0.4	1.1	12.0	0.2	0.0	0.0	0.1	0.0
E-MNIST	35.6	26.4	30.4	34.5	34.7	32.8	14.3	34.2	31.4	35.8	30.6	19.5	12.6	26.8	26.7
K-MNIST	14.4	5.9	7.7	14.0	10.5	8.1	2.1	9.7	8.5	14.5	8.9	6.5	0.7	5.8	5.9
CIFAR-Gr	0.2	0.0	0.0	0.2	0.0	0.0	0.0	0.0	0.0	0.2	0.0	0.0	0.0	0.0	0.0
Uniform	44.3	0.0	19.8	93.1	0.0	0.0	0.0	0.0	0.0	54.2	0.0	0.0	0.0	0.0	0.0
Smooth	0.0	0.0	0.0	0.0	0.0	0.0	0.0	0.0	0.0	0.0	0.0	0.0	0.0	0.0	0.0
F-MNIST															
MNIST	73.5	38.5	65.8	66.8	43.5	10.4	9.5	50.1	57.2	72.2	25.6	3.5	11.5	38.9	39.9
E-MNIST	73.6	21.0	58.6	68.1	18.7	3.0	5.0	34.0	40.6	72.2	6.0	0.5	4.6	14.7	23.1
K-MNIST	73.7	37.4	47.2	62.6	28.0	6.1	10.6	33.4	36.7	71.6	18.2	1.8	8.7	32.5	38.7
CIFAR-Gr	87.2	0.0	86.6	75.3	0.0	0.0	0.0	0.0	0.0	87.7	0.0	0.0	0.0	0.0	0.0
Uniform	81.3	0.0	86.3	87.3	0.0	0.0	0.0	0.0	0.0	81.0	0.0	0.0	0.0	0.0	0.1
Smooth	26.8	0.0	24.2	19.6	0.0	0.0	0.0	0.2	0.1	27.3	0.0	0.0	0.0	0.0	0.0
SVHN															
CIFAR-10	18.9	0.1	9.5	15.0	0.3	0.1	0.2	0.0	0.1	15.4	0.4	0.0	0.0	0.0	0.1
LSUN-CR	19.7	0.0	8.3	17.2	0.0	0.0	0.0	0.0	0.0	15.5	0.0	0.0	0.0	0.0	0.0
CIFAR-100	21.8	0.2	11.6	18.1	0.5	0.2	0.5	0.1	0.2	17.6	0.6	0.1	0.2	0.2	0.1
FMNIST-3D	26.7	0.0	17.5	24.5	0.0	0.0	0.6	0.0	0.0	27.2	0.1	0.0	0.0	0.0	0.0
Uniform	30.0	0.0	6.4	48.2	0.0	0.0	0.0	0.0	0.0	17.0	0.0	0.0	0.0	0.0	0.0
Smooth	17.3	12.0	6.9	9.1	7.7	9.7	9.5	8.3	8.4	10.1	8.1	5.3	5.9	6.6	6.4
CIFAR-10															
SVHN	34.5	10.0	33.9	33.5	30.6	5.3	59.4	18.3	33.9	35.5	12.7	2.6	47.2	8.7	10.8
LSUN-CR	53.3	28.0	44.0	49.4	25.9	8.3	43.7	36.8	34.8	53.8	17.5	1.3	41.2	30.1	28.4
CIFAR-100	61.2	57.8	52.5	58.4	58.5	55.3	63.3	56.8	57.1	61.4	59.6	62.6	62.2	60.4	57.9
FMNIST-3D	42.4	26.8	30.7	37.4	19.0	5.4	43.9	32.2	29.6	43.2	15.4	2.8	36.8	24.2	27.8
Uniform	87.7	0.0	0.0	13.8	0.0	0.0	0.0	0.0	0.0	92.8	0.0	0.0	0.0	0.0	0.0
Smooth	35.1	14.2	32.9	26.4	34.0	8.1	31.9	30.3	23.1	34.9	15.5	2.8	43.6	7.5	14.9
CIFAR-100															
LSUN-CR	82.0	64.3	75.3	73.8	62.3	23.9	76.3	65.3	67.6	82.8	55.9	13.5	75.6	65.3	64.1
CIFAR-10	79.8	81.9	76.4	78.2	81.4	90.9	82.8	79.5	79.0	79.5	80.9	91.4	81.7	80.8	80.0
FMNIST-3D	65.8	58.5	61.8	57.1	41.0	14.0	72.0	51.7	56.0	66.1	58.6	21.1	69.0	59.2	59.3
Uniform	97.6	0.0	94.3	100.0	0.0	0.0	0.0	0.0	0.0	98.8	0.0	0.0	0.0	0.0	0.0
Smooth	79.5	65.2	58.7	79.1	64.8	29.4	80.2	54.4	64.0	79.2	41.6	2.6	78.0	57.1	66.2

Table 6: OOD data detection in terms of AUROC. Higher is better. Values are averages over five prediction runs.

Datasets	MAP	OE	DE	VB						LA					
				Plain	NC1	NC2	SL	ML	OE	Plain	NC1	NC2	SL	ML	OE
MNIST															
F-MNIST	97.3	99.9	98.7	97.4	99.9	100.0	99.9	99.8	99.6	97.4	99.9	100.0	99.9	99.9	99.9
E-MNIST	89.1	93.7	90.4	89.9	90.4	90.7	95.7	91.1	92.1	89.1	91.2	95.6	94.9	93.3	93.6
K-MNIST	96.9	98.5	98.1	96.9	97.8	98.3	98.8	98.0	98.2	96.9	97.9	98.6	99.2	98.5	98.5
CIFAR-Gr	99.6	100.0	99.8	99.6	100.0	100.0	100.0	100.0	100.0	99.6	100.0	100.0	100.0	100.0	100.0
Uniform	95.0	100.0	95.8	90.5	100.0	100.0	100.0	100.0	100.0	94.6	100.0	100.0	100.0	100.0	100.0
Smooth	100.0	100.0	100.0	100.0	100.0	100.0	100.0	100.0	100.0	100.0	100.0	100.0	100.0	100.0	100.0
F-MNIST															
MNIST	79.7	92.9	83.0	85.3	87.9	96.9	98.6	86.7	86.2	80.3	94.2	99.3	98.2	92.9	92.5
E-MNIST	81.8	96.5	87.5	85.1	95.6	99.2	99.2	92.0	91.3	82.3	98.9	99.9	99.3	97.6	96.1
K-MNIST	83.1	94.4	91.7	86.9	94.3	98.6	98.4	93.5	93.3	83.9	96.9	99.5	98.7	94.9	94.1
CIFAR-Gr	82.2	100.0	83.6	87.5	100.0	100.0	100.0	100.0	100.0	81.4	100.0	100.0	100.0	100.0	100.0
Uniform	85.5	100.0	85.7	85.8	100.0	100.0	100.0	100.0	100.0	85.3	100.0	100.0	100.0	100.0	100.0
Smooth	95.7	100.0	96.4	97.2	100.0	100.0	100.0	100.0	100.0	95.5	100.0	100.0	100.0	100.0	100.0
SVHN															
CIFAR-10	96.2	100.0	97.9	95.6	99.9	100.0	99.9	100.0	100.0	97.1	99.9	100.0	100.0	100.0	100.0
LSUN-CR	95.7	100.0	97.7	95.9	100.0	100.0	100.0	100.0	100.0	97.0	100.0	100.0	100.0	100.0	100.0
CIFAR-100	95.5	99.9	97.4	94.7	99.9	99.9	99.8	100.0	99.9	96.5	99.9	100.0	99.9	100.0	100.0
FMNIST-3D	95.5	100.0	97.1	91.4	100.0	100.0	99.8	100.0	100.0	95.6	100.0	100.0	99.9	100.0	100.0
Uniform	94.3	100.0	98.2	80.2	100.0	100.0	100.0	100.0	100.0	96.8	100.0	100.0	100.0	100.0	100.0
Smooth	96.5	97.6	98.4	97.5	97.7	97.0	95.9	97.5	97.7	97.7	98.4	98.8	98.1	98.5	98.7
CIFAR-10															
SVHN	95.6	98.2	95.6	95.7	95.8	98.2	89.0	97.2	95.6	95.5	97.8	98.6	92.7	98.7	98.1
LSUN-CR	91.8	95.9	93.7	91.5	96.1	98.0	92.5	94.1	94.4	92.0	97.5	99.1	93.8	95.7	96.0
CIFAR-100	89.8	90.1	91.3	88.6	88.2	87.6	85.9	88.3	88.9	89.9	89.8	89.0	86.2	89.7	90.0
FMNIST-3D	94.4	96.2	95.8	94.5	97.2	98.6	92.9	95.1	95.9	94.3	97.7	98.9	94.0	96.6	96.1
Uniform	93.0	100.0	99.5	97.6	100.0	100.0	100.0	100.0	100.0	92.2	100.0	100.0	100.0	100.0	100.0
Smooth	94.3	97.6	95.6	96.0	95.3	97.5	94.8	95.4	96.2	94.6	97.6	98.6	93.9	98.8	97.6
CIFAR-100															
LSUN-CR	78.4	85.3	83.8	81.3	87.9	93.0	80.1	85.6	85.3	78.8	89.1	96.9	82.0	86.3	85.9
CIFAR-10	77.4	77.1	79.8	77.7	76.8	74.1	76.3	77.8	77.3	77.8	77.5	70.1	76.6	77.6	77.7
FMNIST-3D	85.3	86.2	87.6	87.7	91.5	96.6	84.0	89.6	87.9	85.2	87.0	96.3	85.7	86.3	86.0
Uniform	80.1	100.0	87.7	64.8	100.0	100.0	100.0	100.0	100.0	82.6	100.0	100.0	100.0	99.9	100.0
Smooth	77.0	76.6	82.9	69.4	74.5	90.5	80.3	83.2	78.3	79.4	91.7	98.7	78.1	86.4	77.7

Table 7: OOD data detection in terms of AUPRC. Higher is better. Values are averages over five prediction runs.

Datasets	MAP	OE	DE	VB						LA					
				Plain	NC1	NC2	SL	ML	OE	Plain	NC1	NC2	SL	ML	OE
MNIST															
F-MNIST	96.9	99.9	98.7	97.5	99.9	100.0	99.8	99.8	99.6	97.0	99.9	100.0	99.9	99.9	99.9
E-MNIST	74.2	86.7	77.2	76.3	77.8	77.3	83.3	80.6	82.5	74.1	79.6	89.8	78.8	85.5	86.4
K-MNIST	96.5	98.5	98.0	96.4	97.5	97.8	97.2	97.8	98.1	96.6	97.8	98.2	98.9	98.4	98.4
CIFAR-Gr	99.7	100.0	99.8	99.6	100.0	100.0	100.0	100.0	100.0	99.6	100.0	100.0	100.0	100.0	100.0
Uniform	96.7	100.0	97.3	93.4	100.0	100.0	100.0	100.0	100.0	96.5	100.0	100.0	100.0	100.0	100.0
Smooth	100.0	100.0	100.0	100.0	100.0	100.0	100.0	100.0	100.0	100.0	100.0	100.0	100.0	100.0	100.0
F-MNIST															
MNIST	75.3	92.2	79.0	83.1	84.0	94.9	98.4	83.9	84.1	76.3	92.5	99.1	98.0	92.3	91.9
E-MNIST	66.9	92.7	76.4	74.0	88.7	97.3	98.2	82.8	82.5	67.8	96.8	99.6	98.4	94.8	92.0
K-MNIST	81.7	94.4	91.1	85.2	93.1	98.1	98.1	92.5	92.6	82.8	96.2	99.5	98.6	94.7	94.2
CIFAR-Gr	85.5	100.0	87.2	89.6	100.0	100.0	100.0	100.0	100.0	84.9	100.0	100.0	100.0	100.0	100.0
Uniform	88.1	100.0	88.9	89.2	100.0	100.0	100.0	100.0	100.0	87.9	100.0	100.0	100.0	100.0	100.0
Smooth	95.3	100.0	96.1	96.9	100.0	100.0	100.0	100.0	100.0	95.1	100.0	100.0	100.0	100.0	100.0
SVHN															
CIFAR-10	98.3	100.0	99.1	96.9	99.9	100.0	99.9	100.0	100.0	98.8	100.0	100.0	100.0	100.0	100.0
LSUN-CR	99.9	100.0	100.0	99.9	100.0	100.0	100.0	100.0	100.0	100.0	100.0	100.0	100.0	100.0	100.0
CIFAR-100	97.7	100.0	98.8	96.4	99.9	100.0	99.9	100.0	100.0	98.3	99.9	100.0	100.0	100.0	100.0
FMNIST-3D	98.1	100.0	98.8	93.5	100.0	100.0	99.9	100.0	100.0	98.2	100.0	100.0	100.0	100.0	100.0
Uniform	97.3	100.0	99.3	82.8	100.0	100.0	100.0	100.0	100.0	98.7	100.0	100.0	100.0	100.0	100.0
Smooth	98.5	98.9	99.4	98.6	98.6	98.0	96.5	98.4	98.7	99.1	99.3	99.5	98.7	99.4	99.5
CIFAR-10															
SVHN	93.3	96.5	93.3	93.3	92.8	96.6	77.6	94.5	92.8	93.3	95.9	97.9	85.2	97.0	96.4
LSUN-CR	99.7	99.8	99.7	99.6	99.8	99.9	99.7	99.7	99.7	99.7	99.9	100.0	99.7	99.8	99.8
CIFAR-100	89.9	90.0	91.3	86.7	85.7	84.2	82.8	85.3	86.9	90.0	90.0	89.1	82.4	89.8	90.0
FMNIST-3D	95.1	96.4	96.1	94.7	97.0	98.5	92.8	95.0	96.1	95.0	97.6	99.0	93.4	96.7	96.3
Uniform	95.5	100.0	99.6	98.0	100.0	100.0	100.0	100.0	100.0	95.0	100.0	100.0	100.0	100.0	100.0
Smooth	94.4	97.5	95.8	95.7	95.5	97.5	93.9	95.1	95.9	94.7	97.6	98.7	93.9	98.6	97.4
CIFAR-100															
LSUN-CR	99.0	99.4	99.3	99.0	99.5	99.7	99.1	99.3	99.3	99.0	99.5	99.9	99.2	99.4	99.4
CIFAR-10	77.2	77.0	79.3	76.8	77.1	73.0	75.4	77.4	77.1	77.3	77.1	68.2	75.8	77.2	77.1
FMNIST-3D	85.7	86.0	88.2	87.6	90.9	96.6	84.8	89.3	87.6	85.6	87.1	96.8	86.5	86.3	85.7
Uniform	84.6	100.0	91.5	73.3	100.0	100.0	100.0	100.0	100.0	87.1	100.0	100.0	100.0	99.9	100.0
Smooth	75.4	71.0	80.3	67.4	69.8	88.1	81.4	79.9	74.9	78.5	90.9	98.8	78.3	85.4	73.9

Table 8: Confidences in terms of MMC, averaged over five prediction runs. Lower is better for OOD datasets.

Datasets	MAP	OE	DE	VB						LA					
				Plain	NC1	NC2	SL	ML	OE	Plain	NC1	NC2	SL	ML	OE
MNIST	99.1	99.4	99.3	98.7	98.2	98.2	99.1	98.2	98.6	99.0	99.3	99.3	99.2	99.2	99.3
F-MNIST	66.3	22.0	64.9	70.4	6.1	6.1	20.4	21.2	27.3	65.2	7.7	7.7	21.0	20.7	22.2
E-MNIST	82.3	79.3	80.9	78.6	74.0	73.9	75.9	73.0	73.9	81.1	79.6	79.6	80.4	76.5	78.1
K-MNIST	73.3	65.7	69.7	67.6	51.8	51.8	61.2	50.3	52.4	71.8	64.3	64.3	66.3	62.3	64.3
CIFAR-Gr	48.0	10.0	43.1	45.2	0.0	0.0	10.0	10.1	10.1	47.3	0.0	0.0	10.1	10.4	10.2
Uniform	96.8	10.0	97.4	97.8	0.1	0.1	10.0	10.1	10.1	96.5	0.0	0.0	10.2	10.3	10.2
Smooth	12.9	10.1	12.6	12.7	0.3	0.3	21.6	10.2	10.2	12.8	0.5	0.5	20.5	10.1	10.1
F-MNIST	96.1	96.0	94.8	93.6	91.0	91.0	95.0	91.2	92.9	95.7	94.9	94.9	93.5	94.5	94.7
MNIST	82.8	60.1	74.3	70.9	50.0	50.0	32.9	57.2	63.7	80.9	33.8	33.8	33.9	55.9	57.9
E-MNIST	82.5	45.0	70.0	71.5	25.0	25.0	25.5	44.4	50.7	80.6	9.4	9.4	24.3	36.2	44.7
K-MNIST	82.5	60.1	64.0	68.4	37.0	37.1	33.5	44.8	48.0	80.0	28.1	28.1	32.0	52.6	57.3
CIFAR-Gr	89.1	10.0	84.6	73.1	0.0	0.0	10.0	10.1	10.2	88.6	0.0	0.0	10.8	10.3	10.3
Uniform	85.5	13.2	82.3	79.4	0.6	0.6	10.2	10.6	11.1	84.2	0.0	0.0	10.9	12.2	15.0
Smooth	48.0	10.5	44.0	42.0	1.0	1.0	11.0	11.9	10.7	47.4	0.3	0.3	11.6	10.4	10.8
SVHN	98.6	98.6	98.1	97.7	97.3	97.3	98.4	97.1	97.6	97.9	98.0	98.0	97.9	97.8	97.3
CIFAR-10	69.0	11.6	57.3	61.3	3.7	3.7	15.4	11.1	11.7	60.7	3.6	3.5	12.4	12.1	12.5
LSUN-CR	69.8	10.2	57.7	63.9	0.1	0.1	10.8	10.2	10.2	61.5	0.0	0.0	11.0	10.3	10.7
CIFAR-100	70.3	12.4	58.8	63.5	4.3	4.3	17.3	11.6	12.3	62.3	4.1	4.1	13.4	12.7	13.4
FMNIST-3D	73.6	11.0	62.5	67.8	1.5	1.5	17.6	10.8	11.5	68.0	1.8	1.8	15.5	10.9	12.0
Uniform	77.5	10.3	57.1	82.2	0.1	0.1	10.0	10.1	10.2	65.7	0.0	0.0	10.4	10.3	10.7
Smooth	68.8	52.1	51.3	55.5	42.3	42.3	62.7	45.6	44.0	58.3	43.9	43.8	44.9	44.6	40.8
CIFAR-10	96.7	96.9	95.9	95.7	94.5	94.5	96.0	95.1	95.5	96.4	94.9	94.9	95.8	96.1	96.1
SVHN	65.2	45.7	60.8	59.5	49.7	49.8	73.3	45.0	55.8	63.5	36.8	36.9	64.7	33.0	44.0
LSUN-CR	73.9	58.7	65.2	68.2	41.1	41.1	64.3	56.7	57.1	71.6	29.2	28.6	61.7	53.6	55.2
CIFAR-100	77.2	76.1	69.8	72.4	67.7	67.7	75.9	69.8	70.5	75.4	67.3	67.3	74.3	73.2	72.6
FMNIST-3D	67.7	55.9	58.5	60.4	32.7	32.7	64.3	54.5	52.3	66.0	27.4	27.3	57.6	48.5	53.1
Uniform	82.1	10.3	40.7	52.2	0.1	0.1	10.2	10.7	10.1	81.9	0.0	0.0	10.2	10.3	10.3
Smooth	64.3	45.2	57.2	54.0	51.4	51.5	53.3	53.0	49.3	62.5	32.6	32.7	59.5	26.4	43.5
CIFAR-100	84.7	85.1	80.9	69.0	66.2	66.2	80.1	67.1	67.1	81.6	80.3	80.3	77.0	79.1	79.4
SVHN	52.8	43.9	43.8	27.3	31.0	30.9	46.2	24.9	26.9	46.9	33.7	33.8	42.1	34.8	37.9
LSUN-CR	62.7	51.3	48.8	33.3	21.1	21.2	49.7	26.5	26.4	57.0	36.4	36.3	43.5	40.9	42.6
CIFAR-10	62.9	63.7	53.4	39.0	36.9	36.9	55.3	37.2	37.4	57.3	55.7	55.6	50.8	53.8	54.0
FMNIST-3D	51.8	48.2	42.5	24.8	15.9	15.9	44.5	20.6	22.6	47.1	40.7	40.8	38.4	40.3	41.4
Uniform	64.2	1.4	45.0	59.4	0.0	0.0	2.2	1.2	1.2	54.4	0.0	0.0	1.5	4.4	1.5
Smooth	61.7	58.9	47.3	49.3	38.4	38.5	50.6	28.7	34.8	54.8	30.4	30.5	49.1	40.2	51.5

Table 9: OOD data detection under models trained with random noises (Hein et al., 2019) as \mathcal{D}_{out} . Values are FPR95, averaged over ten prediction runs—lower is better.

Datasets	MAP	OE	DE	VB						LA					
				Plain	NC1	NC2	SL	ML	OE	Plain	NC1	NC2	SL	ML	OE
MNIST															
F-MNIST	11.8	6.8	5.3	12.5	6.5	6.5	0.6	11.9	10.3	12.0	8.2	4.3	0.0	6.3	6.8
E-MNIST	35.6	30.7	30.4	34.5	35.1	42.4	17.9	37.3	34.3	35.8	34.2	39.2	15.3	31.0	30.7
K-MNIST	14.4	7.8	7.7	14.0	14.5	17.1	1.1	15.8	14.0	14.5	10.6	9.5	0.7	8.5	7.8
CIFAR-Gr	0.2	0.0	0.0	0.2	0.0	0.0	0.0	0.0	0.1	0.2	0.0	0.0	0.0	0.0	0.0
Uniform	44.3	0.7	19.8	93.1	0.0	0.0	0.0	1.9	1.8	54.2	0.7	0.0	0.0	0.6	0.8
F-MNIST															
MNIST	73.5	62.2	65.8	66.8	62.2	34.6	30.4	59.1	60.4	72.2	60.8	13.8	24.3	55.4	57.4
E-MNIST	73.6	50.2	58.6	68.1	43.9	13.0	25.7	54.7	54.6	72.2	44.2	3.3	22.5	39.6	48.3
K-MNIST	73.7	47.4	47.2	62.6	31.4	8.2	19.1	35.6	38.1	71.6	33.9	2.9	20.9	31.7	43.0
CIFAR-Gr	87.2	0.5	86.6	75.3	0.1	0.0	0.2	0.8	1.1	87.7	0.7	0.0	0.2	0.7	1.0
Uniform	81.3	26.0	86.3	87.3	47.1	0.6	0.0	0.2	4.9	81.0	43.4	0.0	0.0	22.0	38.1
SVHN															
CIFAR-10	18.9	13.8	9.5	15.0	13.0	14.5	16.5	8.4	11.5	15.4	8.4	18.7	94.8	14.9	11.4
LSUN-CR	19.7	9.0	8.3	17.2	10.5	8.8	8.8	5.4	9.1	15.5	8.3	3.5	95.4	12.6	8.2
CIFAR-100	21.8	15.6	11.6	18.1	14.8	16.4	17.9	10.2	12.4	17.6	11.6	21.4	93.9	16.6	13.4
FMNIST-3D	26.7	29.8	17.5	24.5	31.1	34.8	30.4	30.0	25.3	27.2	34.6	70.5	95.1	23.3	27.7
Uniform	30.0	0.0	6.4	48.2	0.0	0.0	0.0	0.0	0.0	17.0	0.0	0.0	90.2	19.0	0.0
CIFAR-10															
SVHN	34.5	7.3	33.9	33.5	11.1	3.8	20.6	11.0	9.7	35.5	6.6	0.8	26.0	7.5	8.3
LSUN-CR	53.3	49.0	44.0	49.4	46.7	35.0	61.7	45.7	47.6	53.8	48.9	27.8	54.9	51.9	48.3
CIFAR-100	61.2	58.2	52.5	58.4	57.7	49.6	71.1	56.3	56.6	61.4	59.3	49.4	70.7	57.6	59.0
FMNIST-3D	42.4	44.9	30.7	37.4	39.4	24.3	62.7	43.3	44.0	43.2	40.2	14.1	57.8	40.8	46.4
Uniform	87.7	26.7	0.0	13.8	100.0	100.0	57.3	98.0	100.0	92.8	3.5	0.0	17.7	12.9	49.8
CIFAR-100															
LSUN-CR	82.0	79.7	75.3	73.8	80.9	83.9	91.5	77.9	71.1	82.8	82.0	85.3	78.5	72.8	79.7
CIFAR-10	79.8	80.5	76.4	78.2	81.3	86.9	93.9	80.0	81.4	79.5	80.6	88.9	82.1	78.8	80.2
FMNIST-3D	65.8	66.9	61.8	57.1	69.3	42.1	93.6	63.1	61.9	66.1	71.2	60.8	82.0	64.4	67.9
Uniform	97.6	73.3	94.3	100.0	99.7	49.5	95.4	99.5	99.8	98.8	88.4	100.0	100.0	88.9	54.0

Table 10: OOD data detection on text classification tasks. Values are FPR95, averaged over five prediction runs—lower is better.

Datasets	MAP	OE	DE	LA					
				Plain	NC1	NC2	SL	ML	OE
SST									
SNLI	100.0	0.0	100.0	100.0	0.0	0.0	97.0	89.6	0.0
Multi30k	100.0	0.0	100.0	100.0	0.0	0.0	99.5	83.5	0.0
WMT16	100.0	0.0	100.0	100.0	0.0	0.0	89.3	80.7	0.0
20NG									
SNLI	0.0	0.0	0.0	0.0	0.0	0.0	0.0	0.0	0.0
Multi30k	0.0	0.0	0.4	0.0	0.0	0.0	0.0	0.0	0.0
WMT16	0.0	0.0	1.3	0.1	0.0	0.0	0.0	0.0	0.0
TREC									
SNLI	99.7	0.0	31.0	99.7	0.0	0.0	0.7	0.0	0.0
Multi30k	100.0	0.0	14.2	100.0	0.0	0.0	0.8	0.0	0.0
WMT16	89.2	0.0	27.3	89.3	0.0	0.0	0.8	0.0	0.0